

Real-time Vision-based UAV Navigation in Fruit Orchards

Dries Hulens, Maarten Vandersteegen and Toon Goedemé
EAVISE, KU Leuven, Jan de Nayerlaan 5, Sint-Katelijne-Waver, Belgium
{dries.hulens, maarten.vandersteegen, toon.goedeme}@kuleuven.be

Keywords: Unmanned Aerial Vehicle, Agriculture, Orchard, Vision-based Navigation.

Abstract: Unmanned Aerial Vehicles (UAV) enable numerous agricultural applications such as terrain mapping, monitor crop growth, detecting areas with diseases and so on. For these applications a UAV flies above the terrain and has a global view of the plants. When the individual fruits or plants have to be examined, an oblique view is better, e.g. via an inspection-camera mounted on expensive all-terrain wheeled robots that drive through the orchard. However, in this paper we aim to autonomously navigate through the orchard with a low-cost UAV and cheap sensors (e.g. a webcam). Evidently, this is challenging since every orchard or even every corridor looks different. For this we developed a vision-based system that detects the center and end of the corridor to autonomously navigate the UAV towards the end of the orchard without colliding with the trees. Furthermore extensive experiments were performed to prove that our algorithm is able to navigate through the orchard with high accuracy and in real-time, even on embedded hardware. A connection with a ground station is thus unnecessary which makes the UAV fully autonomous.

1 INTRODUCTION

Nowadays drones are used in many applications such as search and rescue, inspection of buildings, performing 3D reconstructions and so. A fairly new application is fruit growth estimation in orchards. By regularly inspecting the fruit orchard, diseases can be detected in an early state. This avoids the need to fully spray the entire orchard and only the infected trees can be treated. Obviously this is a time-consuming task for the farmer and therefore not feasible. In this paper we propose a vision-based technique to steer a UAV (Unmanned Aerial Vehicle) autonomously through an orchard. Techniques to count fruit in an orchard (Puttemans et al., 2016) or to detect diseases on fruit are already widely discussed in literature (Garcia-Ruiz et al., 2013; Spadaro and Gullino, 2004) and therefore we focus on the navigation part. A UAV has four DOF (Degrees Of Freedom) as shown in figure 1. The pitch causes the UAV to go forward or backward, the roll is used to go to the left or right, the yaw rotates the UAV around its vertical axis and the thrust is used to control the altitude.

To fly autonomously through an orchard the UAV is equipped with a frontal looking camera and on-board processing. The camera captures images of the corridor and passes these to the on-board processing board which processes the images and controls the

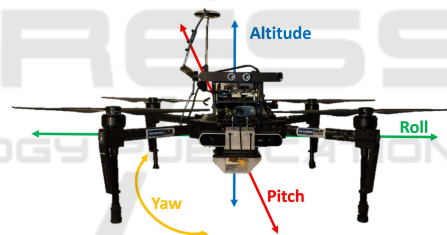


Figure 1: Matrice M100 from DJI with a Logitech C310 webcam and Barebone Brix mini computer.

UAV accordingly. To fly through the orchard without colliding with the trees the UAV should always fly in the middle of two tree lines, facing the end of the corridor. Accordingly, the middle and end of the corridor is detected by our algorithm which is used to control the roll (to stay in the center of the corridor) and the yaw (to face the UAV to the end of the corridor).

When the end of the corridor is reached, one of the possibilities is to use GPS to fly to the next corridor, but this is not covered in this paper. The UAV that we are using is a Matrice M100 (see figure 1) from DJI equipped with a Brix mini computer containing an Intel i7 processor and 8GB RAM. The flight controller that we use is the N1 also from DJI. We also ran our algorithm on two smaller Odroid processing platforms containing a Samsung Exynos4412 and a Samsung Exynos5422 processor with 2GB of RAM which only weigh approximately 52 and 70 grams. These



Figure 2: An example of an orchard. Blue point is the CP of corridor and purple point is the VP of the corridor.

platforms can be mounted on even smaller UAVs.

The remainder of this paper is structured as follows; in Section 2 we relate our method with the current literature. In Section 3 we explain how we detect the vanishing point and center point of the corridor to correct the yaw and roll of the UAV during flight. In Section 4 our results are discussed and in Section 5 conclusions are drawn and future work is discussed.

2 RELATED WORK

As discussed in (Pajares, 2015) UAVs are used in a lot of applications and carrying different sensors to extract information out of their environment.

UAVs are more and more used to fly over fields in open space for constructing a (3D)map for precision agriculture as in (Zarco-Tejada et al., 2014) where they monitor plant growth. Also diseases can be detected in an early state by a UAV flying over the terrain as in (Garcia-Ruiz et al., 2013) where a hyperspectral camera is mounted on the UAV to find abnormalities in citrus trees. In (Colomina and Molina, 2014) an overview is given of different photogrammetry and remote sensing techniques.

In (Puttemans et al., 2016) software was developed to detect and count fruit from images taken from a camera mounted on a wheeled robot for early harvest estimation. When a more accurate view of the fruit is needed generally wheeled robots are used that can drive through the orchard like in (Christiansen et al., 2011; Barawid et al., 2007; Andersen et al., 2010; Hiremath et al., 2014) where they use a LIDAR combined with other sensors like GPS to drive through the orchard. Or in (Rovira-Más et al., 2008) where stereo vision is used to make a 3D map of the orchard with a wheeled robot. The disadvantage of these robots is that they are all carrying a heavy and expensive laser scanner. In (Xue et al., 2012) vision-

based techniques are used to find the path between the trees. Here a simple color segmentation is used to distinguish the path from the corn plants. Of course, still a very expensive wheeled robot is needed that requires frequent maintenance.

Navigating through an orchard with a UAV instead of a wheeled vehicle has multiple advantages. The slope and condition of the path is not that important as when using a wheeled robot. Furthermore, a UAV flies much faster and the cost of a UAV and its maintenance is much lower than with a wheeled robot.

Initial experiments with UAVs flying through an orchard were already performed by (Verbeke et al., 2014) where they designed a UAV-frame specifically to fly in fruit orchards, which can be equipped with a small computer and cameras. In (Stefas et al., 2016), they experimented with a monocular and binocular camera to retrieve the path between the tree rows. Unfortunately, their algorithm is based on a traffic lane detection algorithm and results in a poor classification of the tree rows.

We developed a new approach to navigate through an orchard using a cheap webcam and on-board processing. Our approach has a high accuracy both in finding the center and the end of the corridor. No expensive laser scanner or robot is needed and our system can be used in multiple types of orchards.

3 APPROACH

When a human is walking through an orchard he follows the path to avoid collisions with the trees. Two actions are taking place; 1. The human tries to stay in the middle of the path, 2. The human looks to the end of the corridor to walk in a straight line. The same is true for a UAV, the roll should be controlled to stay in the center of the path and the yaw to keep the nose of the UAV pointing towards the end of the corridor. Evidently, the pitch is steered at a fixed speed to go forward and the altitude is maintained stable.

To control these two DOF, the roll and yaw, we developed an algorithm that estimates the center of the corridor (CP, center point) and the end of the corridor (VP, vanishing point). The algorithm is designed to estimate these two points in a computational low-cost-manner so they are able to run in real-time on embedded hardware, mounted on the UAV. Figure 3 shows the overall system where the CP and the VP are found. In section 3.1 we first show how we estimate the CP and in section 3.2 we explain how the VP is found.

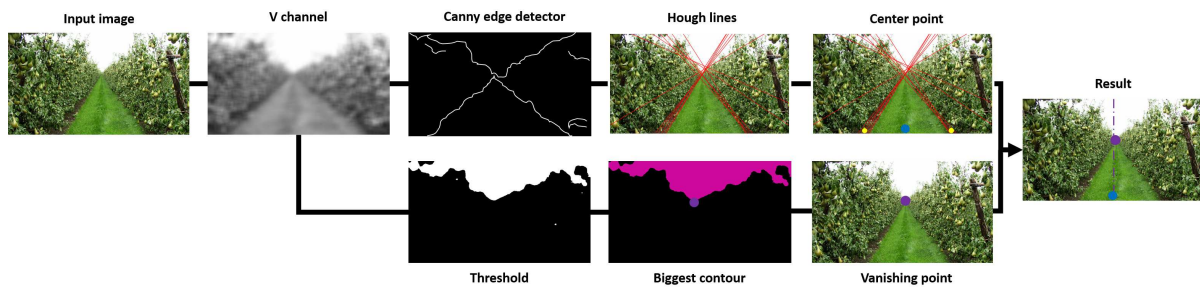


Figure 3: Overall system. Upper part: center point detection. Lower part: vanishing point detection.

3.1 Center Point Estimation

As seen in figure 4 the center of the corridor (blue) is found between the intersections (red) of the boundaries of the grass path (yellow) and the horizontal axis on the bottom of the input image. At first sight the color transition between the path and trees could be used to detect these intersections but experiments in multiple types of orchards show that the color of the path and trees differs a lot. Therefore we used the difference in brightness between trees and path which will always be visible regardless the type of orchard. The brightness is found by converting the input image from RGB to HSV. The V channel (value) represents the brightness of the image as seen in figure 3 where the grass, trees and sky are easily distinguishable.

Next, a Canny edge detector is used to detect the changes in brightness (borders between trees and path and trees and sky). On this result a Hough line detector is used to detect straight lines which results in figure 3 (Hough lines).

Finally the intersections between the Hough lines and the bottom horizontal axis are calculated and an average is found for the left and right intersection as in figure 3 (Center point - yellow dots). The center point is now found in between the two intersections. As seen, Hough lines are also found between the trees and sky because of the difference in brightness. However they do not affect the result since they don't intersect with the bottom horizontal axis.

To correct the position of the UAV to the center of the corridor, the error between the center of the image and the center of the corridor is used.

3.2 Vanishing Point Detection

To fly through an orchard the nose of the UAV has to point towards the end of the corridor. Therefore the yaw of the UAV should be automatically controlled to point that way. We could use the intersections of the previously found Hough lines which intersect with each other more or less at the end of the corridor to

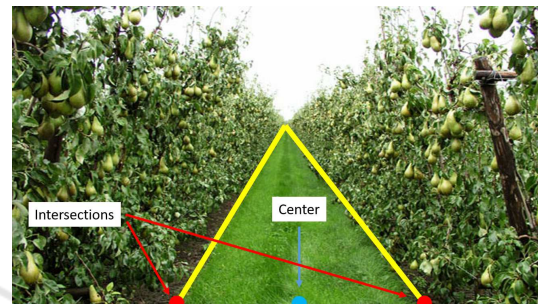


Figure 4: Yellow: Borders of the grass path. Red: Intersection of the borders with the horizontal axis of the frame. Blue: The center of the intersections and also the center of the path called the center point (CP).

estimate the VP. However, in cases where a lot of lines are found in the trees (which have little effect on the CP) the VP is not estimated correctly as illustrated in figure 5. Here the VP is the mean of all Hough line intersections and is indicated in blue where the real VP is indicated in green. To estimate the VP in a more accurate way we make use of the fact that the sky is always brighter than the trees and grass.

We dynamically threshold the V channel of the input image (see figure 3) to separate the sky from the rest of the image. Due to the light shining through the leaves some bright spots occur besides the sky. To neglect these bright spots a *biggest contour finding algorithm* is used to only keep the sky in the image as in figure 3. Due to the shape of a corridor, the sky always looks like a triangle pointing down where the tip of the triangle (lowest point of the contour) represents the end of the corridor and thereby corresponds to the VP. Here the error between the VP and the center of the frame is used to correct the yaw of the UAV. The assumption of the triangular shape of the sky is no longer true at the end of the corridor, which is not an issue in our case since here GPS is used to navigate to the beginning of the next corridor.

To ensure a smooth flight the position of the VP and the CP are filtered with a Kalman filter (Kalman, 1960). When a frame occurs where the VP or the CP cannot be found, the Kalman filters' prediction is used

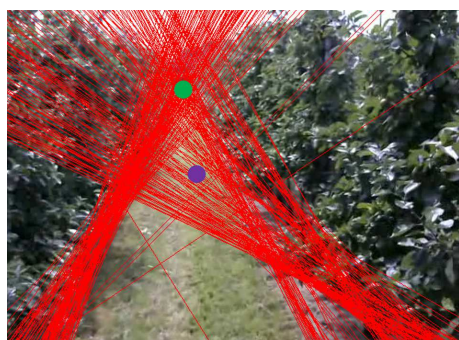


Figure 5: Red: Lines found by Hough Lines algorithm. Purple: Mean of all intersections of the Hough lines. Green: Real vanishing point (VP).

instead.

There is no need for calibrating the camera w.r.t. the UAV before each flight, although the camera should be mounted looking as straight ahead as possible. Small misalignments of the camera can cause the UAV to not position itself exactly in the center of the corridor or not looking perfectly to the VP.

4 EXPERIMENTS AND RESULTS

We performed extensive experiments on 10 different video sequences captured by a UAV flying (manually) through an orchard, adding up to a dataset of 6026 frames in total. In each video sequence 60 frames were randomly selected, yielding 600 frames to evaluate. In each frame the CP and the VP was annotated and compared with the results of our algorithm. Figure 6 shows qualitative results of the output of our algorithm.

4.1 Center Point Experiments

In our experiments we measured the error between the annotated CP and the estimated CP (without Kalman filtering). This error is measured in pixels on the horizontal axis. The maximum allowed error that the UAV can fly to the left or right before colliding with the trees is the half of the width of the path ($0.75m$). The width of the path in the image (expressed in pixels) is changing according to the altitude of the UAV. The lower the UAV flies the larger the width of the path is in the image. Consequently we took the worst case scenario where the UAV flies at $2m$ height and the path is approximately 200 pixels wide. This means that the maximal error is 100 pixels (or $0.75m$) in both directions. In figure 7 the cumulative error is plotted with respect to the percentage of samples (frames).

As seen the average error is $0.17m$ (green dot) and

almost 60% of the samples has a lower error. The average error is considerably smaller than the maximal error of $0.75m$ which means that our algorithms succeeds successfully in finding the center of the corridor.

4.2 Vanishing Point Experiments

We conducted the same experiment to evaluate the correctness of the estimated vanishing point. The difference here is that it is difficult to state a maximum allowed error. When the error is more than 320 pixels (half of the frame width) the VP is no longer visible and retrievable. The Field of view of the camera is 60° which corresponds to 640 pixels yielding a maximal yaw error of 30° .

In figure 8 the cumulative error is plotted w.r.t. the amount of frames. As seen the average error (green dot) is only 0.75° and almost 70% of the samples have an even lower error. Without correcting for this error, the maximal distance that the UAV still can fly, is calculated as seen in figure 9. The maximal distance the UAV can fly before it collides with the trees is $57.7m$. Normally this is impossible since in every frame a new vanishing point is estimated and corrected.

This is an excellent result and proves that our algorithm is capable of detecting the vanishing point with very high accuracy.

4.3 Speed Test on Embedded Hardware

We developed a vision-based algorithm to detect the end and center of a corridor in a fruit orchard. This algorithm yields a frame-rate of more than 30fps on a Brix mini computer (Intel i7, 8GB RAM) mounted on our UAV. This UAV is preprogrammed to fly at a maximal speed of $1m/s$ through the orchard. This means that every 3.3cm the VP and the CP is detected and the UAV its yaw angle and roll is corrected. Evidently we want the algorithm to run in real-time on even smaller embedded computers that can be mounted on small UAVs. We did experiments with two such embedded computers; an Odroid U3 (Samsung Exynos4412, 2GB RAM) and a Odroid XU3 (Samsung Exynos 5422, 2GB RAM) computer. On the Odroid U3 the algorithm runs at 8fps and on the Odroid XU3 at 12fps. This implies that every 12.5cm (U3) and 8.3cm (XU3) the course of the UAV will be corrected. The speed of the algorithm can be further increased (for faster flying UAVs) by using the prediction of the Kalman filter between detections results.



Figure 6: Qualitative results of the output of our algorithm. Blue: the CP, Purple: the VP.

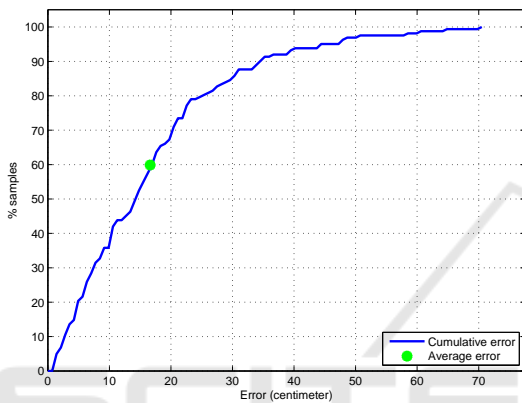


Figure 7: Center point cumulative error. For each error value the percentage of all frames with equal or lower error rate is given. The average error is displayed with a green dot. The maximal allowed error is 0.75m.

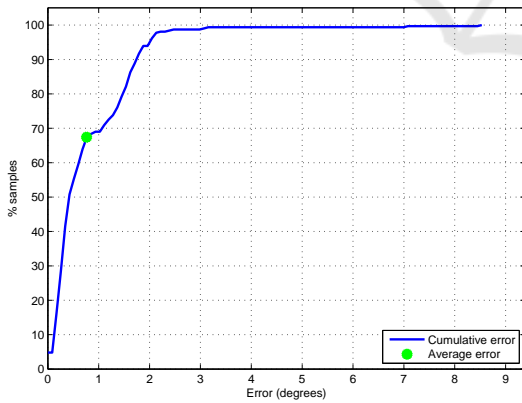


Figure 8: Vanishing point cumulative error. For each error value the percentage of all frames with equal or lower error rate is given. The average error is displayed with a green dot. The maximal allowed error is 30°.

5 CONCLUSIONS AND FUTURE WORK

We developed a lightweight (in terms of processing power) vision-based algorithm to navigate a UAV au-

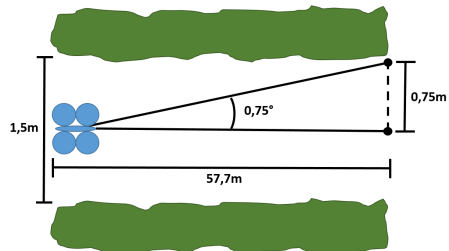


Figure 9: When the average yaw error is 0.75° and the half of the width of the path is 0.75m, the maximum distance the UAV can fly, before colliding with trees, is 57.7m. This is in worst case when in every frame the same average error should be present.

tonomously through a fruit orchard. The center of the corridor is successfully estimated to position the UAV between the trees as well as the vanishing point to align the nose of the UAV with the end of the corridor. Furthermore extensive experiments were performed to evaluate the accuracy of both the *center point* detection and *vanishing point* detection algorithms. These experiments prove that our algorithm is capable of guiding the UAV through the orchard with high precision using only a camera and a small processing board. In addition speed tests were performed to evaluate the real-time character of our algorithm. In https://youtu.be/t5gw_WIUkr4 real-life experiments were performed with an older UAV. In the first part of the video the overall system is shown, in the second and third part the roll and yaw control loops are individually tested. In the future additional outdoor experiments will be performed with the Matrice M100 and a second camera will be added to inspect the fruit.

ACKNOWLEDGEMENTS

This work is supported by KU Leuven via the CAMETRON project.

REFERENCES

- Andersen, J. C., Ravn, O., and Andersen, N. A. (2010). Autonomous rule-based robot navigation in orchards. *IFAC Proceedings Volumes*, 43(16):43–48.
- Barawid, O. C., Mizushima, A., Ishii, K., and Noguchi, N. (2007). Development of an autonomous navigation system using a two-dimensional laser scanner in an orchard application. *Biosystems Engineering*, 96(2):139–149.
- Christiansen, M. P., Jensen, K., Ellekilde, L.-P., and Jørgensen, R. N. (2011). Localization in orchards using extended Kalman filter for sensor-fusion-a frobomind component.
- Colomina, I. and Molina, P. (2014). Unmanned aerial systems for photogrammetry and remote sensing: A review. *ISPRS Journal of Photogrammetry and Remote Sensing*, 92:79–97.
- Garcia-Ruiz, F., Sankaran, S., Maja, J. M., Lee, W. S., Rasmussen, J., and Ehsani, R. (2013). Comparison of two aerial imaging platforms for identification of huanglongbing-infected citrus trees. *Computers and Electronics in Agriculture*, 91:106–115.
- Hiremath, S. A., Van Der Heijden, G. W., Van Evert, F. K., Stein, A., and Ter Braak, C. J. (2014). Laser range finder model for autonomous navigation of a robot in a maize field using a particle filter. *Computers and Electronics in Agriculture*, 100:41–50.
- Kalman, R. E. (1960). A new approach to linear filtering and prediction problems. *Journal of basic Engineering*, 82(1):35–45.
- Pajares, G. (2015). Overview and current status of remote sensing applications based on unmanned aerial vehicles (uavs). *Photogrammetric Engineering & Remote Sensing*, 81(4):281–329.
- Puttemans, S., Vanbrabant, Y., Tits, L., and Goedemé, T. (2016). Automated visual fruit detection for harvest estimation and robotic harvesting. In *IPTA2016*. IEEE.
- Rovira-Más, F., Zhang, Q., and Reid, J. F. (2008). Stereo vision three-dimensional terrain maps for precision agriculture. *Computers and Electronics in Agriculture*, 60(2):133–143.
- Spadaro, D. and Gullino, M. L. (2004). State of the art and future prospects of the biological control of postharvest fruit diseases. *International journal of food microbiology*, 91(2):185–194.
- Stefas, N., Bayram, H., and Isler, V. (2016). Vision-based UAV navigation in orchards. *IFAC-PapersOnLine*, 49(16):10–15.
- Verbeke, J., Hulens, D., Ramon, H., Goedemé, T., and De Schutter, J. (2014). The design and construction of a high endurance hexacopter suited for narrow corridors. In *Unmanned Aircraft Systems (ICUAS), 2014 International Conference on*, pages 543–551. IEEE.
- Xue, J., Zhang, L., and Grift, T. E. (2012). Variable field-of-view machine vision based row guidance of an agricultural robot. *Computers and Electronics in Agriculture*, 84:85–91.
- Zarco-Tejada, P. J., Diaz-Varela, R., Angileri, V., and Loudjani, P. (2014). Tree height quantification using very high resolution imagery acquired from an unmanned aerial vehicle (UAV) and automatic 3D photo-reconstruction methods. *European journal of agronomy*, 55:89–99.